

Yu.S. Proidak, V.A. Gladkykh, A.V. Ruban, O.O. Riabtsev

INVESTIGATION OF PHASE EQUILIBRIA IN THE $\text{MnO}-\text{Al}_2\text{O}_3$ SYSTEM BY DIFFERENTIAL SCANNING CALORIMETRY METHOD

Ukrainian State University of Science and Technologies, Dnipro, Ukraine

All slag from the production of manganese ferroalloys can be conditionally attributed to the system $\text{MnO}-\text{CaO}-\text{SiO}_2-\text{Al}_2\text{O}_3$, since the sum of these oxides reaches 95–98% with MnO content from 18% to 48%. On the practical side, it is crucial to know the peculiarities of the behavior of silicate systems over a wide temperature range and in the presence of various additives. Differential scanning calorimetry was employed to study concentration–temperature transformations in melts corresponding to manganese aluminate, the low-temperature eutectic E1, and a manganese-rich region with 10% Al_2O_3 content. The conducted research indicates a congruently melting nature of manganese spinel MnAl_2O_4 . The preservation of short-range order during the melting of MnAl_2O_4 affects the thermodynamic stability parameters of the compound and the temperature at the onset of manganese recovery during carbothermic reduction. The congruent melting of manganese spinel implies the presence of a second eutectic E2, positioned between MnAl_2O_4 and Al_2O_3 . According to experimental data, the melting temperature of eutectic E2 is lower, approximately 1720°C.

Keywords: manganese ferroalloys, phase equilibrium, $\text{MnO}-\text{Al}_2\text{O}_3$ system, differential scanning calorimetry, differential thermal analysis, spinel.

DOI: 10.32434/0321-4095-2025-162-5-110-116

Introduction

Phase equilibrium in the $\text{MnO}-\text{Al}_2\text{O}_3$ system affects technological parameters of smelting manganese ferroalloys and high-manganese steels. All slag from the production of manganese ferroalloys can be conditionally attributed to the pseudo-quaternary system $\text{MnO}-\text{CaO}-\text{SiO}_2-\text{Al}_2\text{O}_3$, since the sum of these oxides reaches 95–98% with MnO content from 18% to 48%. At the same time, the slag basicity ratio, utilized in practical applications as $\text{CaO}:\text{SiO}_2$, varies from 1:3 to 3:2, and $\text{MnO}:\text{SiO}_2$ ranges from 1:3 to 2:1. The presence of Al_2O_3 in the slag melt depends on the type of ore used, and its content ranges from 3 to 12%. In recent years, the basicity of slags when smelting manganese ferroalloys has been

characterized by different oxide ratios using a comprehensive approach that considers almost all oxides present in the slag, and is expressed by the ratio (%): CaO/SiO_2 , MnO/SiO_2 , $(\text{CaO}+1.4\text{MgO}+\text{MnO})/\text{SiO}_2$, $(\text{CaO}+1.4\text{MgO}+\text{MnO})/(\text{SiO}_2+\text{Al}_2\text{O}_3)$ [1]. The effect of Al_2O_3 concentration and temperature on phase equilibria is of theoretical and practical interest. On the practical side, it is crucial to know the peculiarities of the behavior of silicate systems under a wide temperature range and in the presence of various additives. The recent use of ores with high Al_2O_3 content in the smelting of manganese ferroalloys requires a more detailed analysis of the $\text{MnO}-\text{Al}_2\text{O}_3$ system.

© Yu.S. Proidak, V.A. Gladkykh, A.V. Ruban, O.O. Riabtsev, 2025



This article is an open access article distributed under the terms and conditions of the Creative Commons Attribution (CC BY) license (<https://creativecommons.org/licenses/by/4.0/>).

Yu.S. Proidak, V.A. Gladkykh, A.V. Ruban, O.O. Riabtsev

Experimental

Since manganese ores mainly contain low levels of Al_2O_3 , the literature provides insufficient coverage of the influence of Al_2O_3 on the equilibrium processes in the $\text{MnO}-\text{Al}_2\text{O}_3$ system. However, in recent years, ores with a high Al_2O_3 content have been increasingly used. Additionally, according to refs. [2–4], the $\text{MnO}-\text{Al}_2\text{O}_3$ system is represented by two equilibrium state diagrams (Fig. 1). However, while the low-temperature part of the diagram practically coincides, there are significant differences in the high-temperature region.

According to ref. [2], the $\text{MnO}-\text{Al}_2\text{O}_3$ diagram indicates two eutectics: E1, which occurs at 24% Al_2O_3 with a melting temperature of $1520 \pm 10^\circ\text{C}$, and E2, occurring at 28% MnO with a melting temperature of $1770 \pm 15^\circ\text{C}$. Per the data provided, spinel MnAl_2O_4 melts without decomposition (congruently) at a temperature of $1850 \pm 15^\circ\text{C}$. According to ref. [5], the diagram shows a single eutectic, E1. At that, the MnAl_2O_4 compound melts with decomposition (incongruently) at a lower temperature of 1720°C . Upon reaching this temperature, the forming MnAl_2O_4 compound decomposes into free Al_2O_3 and a melt. The different nature of melting and the release of free Al_2O_3 can affect the properties of the melt. Considering the influence of Al_2O_3 on the thermodynamic aspects of manganese and silicon reduction during the smelting of manganese alloys, as well as its increased content during high silicon recovery at the smelting of high-silicon (MhC25) and commercial ferrosilicon manganese (MhC17) using briquetted charge [5–7], we have employed differential scanning calorimetry

(DSC) [8] to study concentration-temperature transformations in melts (Table 1) corresponding to manganese aluminate (No. 3), the low-temperature eutectic E1 (No. 2), and a manganese-rich region with 10% Al_2O_3 content (No. 1).

Differential scanning calorimetry is employed to determine phase transition temperatures, melting, and crystallization temperatures for individual compounds and their mixtures. In this regard, the capabilities, accuracy, reproducibility of results, data processing and interpretation, phase identification are significantly more reliable compared to differential thermal analysis method (DTA) [8].

The study was conducted using a DSC module, measuring the local differential temperature of the cell (Fig. 2). The differential scanning calorimetry apparatus operated in the temperature sheath scanning mode. The operating temperature range was 400°C to 2080°C , with a possible heating rate ranging from $5^\circ\text{C}/\text{min}$ to $100^\circ\text{C}/\text{min}$. The calibration factor of the apparatus is $20 \mu\text{V}/\text{mW}$ with a relative error of $\pm 0.5\%$, and it is independent of the sample mass. The noise level is $\pm 0.5 \mu\text{V}$. The weight of the sample was 6 g.

The samples were crushed, pressed into a pellet, and then heated in a helium atmosphere at an automatically specified rate of $50 \text{ mV}/\text{h}$ in alundum crucibles that had been precalcined in a neutral atmosphere and reinforced with molybdenum foil. After melting, the samples were kept for 30 min. Then, the cooled samples were crushed to 0.2–0.4 mm, placed in a block, attached to a differential thermocouple, and heated. During the first heating, the readings were not recorded. The measurements were carried out under cooling and subsequent heating. If necessary, without dismantling the block, heating and cooling were repeated to verify the consistency of the results.

Results and discussion

The nature of the transformations and their temperature range are shown in Table 2 and Figs. 3 and 4. When comparing the experimental findings with the data [2,5] for the state diagram $\text{MnO}-\text{Al}_2\text{O}_3$ (Fig. 1), it is worth noting the satisfactory agreement of the obtained results for the high-

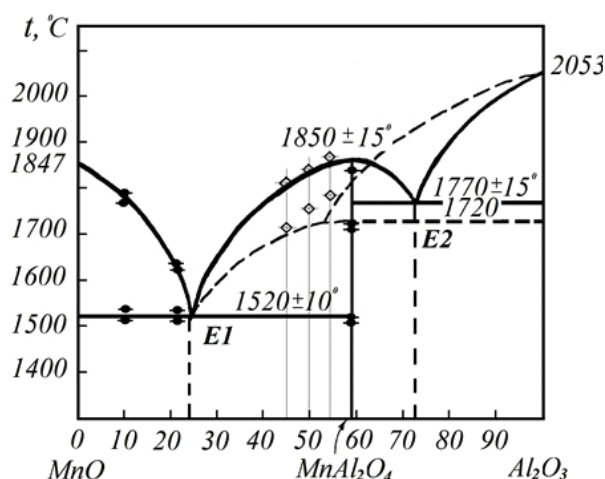


Fig. 1. Equilibrium state diagram of the $\text{MnO}-\text{Al}_2\text{O}_3$ system according to various data: solid line – ref. [2]; dashed line – ref. [5]; ● – results of our own experimental research; ◇ – calculated data

Table 1

Chemical composition of model samples of the $\text{MnO}-\text{Al}_2\text{O}_3$ system using DSC

Sample No.	Chemical composition, %	
	MnO	Al_2O_3
1	90.0	10.0
2	78.2	21.8
3	41.0	59.0

manganese region on both diagrams.

For MnAl_2O_4 , the experimental results are closer to the data [2] in terms of liquidus temperature and coincide with the data [5] for the solidus temperature. The melting range between the solidus and liquidus lines is about 80 degrees, which aligns with the data [5].

Since the melting point of a system decreases when two pure oxides are mixed, precise temperature determination enables the identification of theoretically equilibrium compounds and the amount of impurities within the pure phase. Alternatively, with a known composition, it allows for the prediction of the melting point.

To ensure the proper interpretation of results and provide approximate control over the experiment in the $\text{MnO}-\text{Al}_2\text{O}_3$ binary system, we performed melting temperature calculations for mixtures compositionally similar to the samples using two methods.

In the first method, calculations were performed using the Raoul-Van't Hoff equation [9]:

$$X_2 = A \cdot \Delta T; A = \frac{\Delta H_f}{RT_0^2}; \quad (1)$$

$$X_{2(\text{mol.}\%)} = 100 \cdot \frac{\Delta H_f}{RT_0^2} \cdot \Delta T, \quad (2)$$

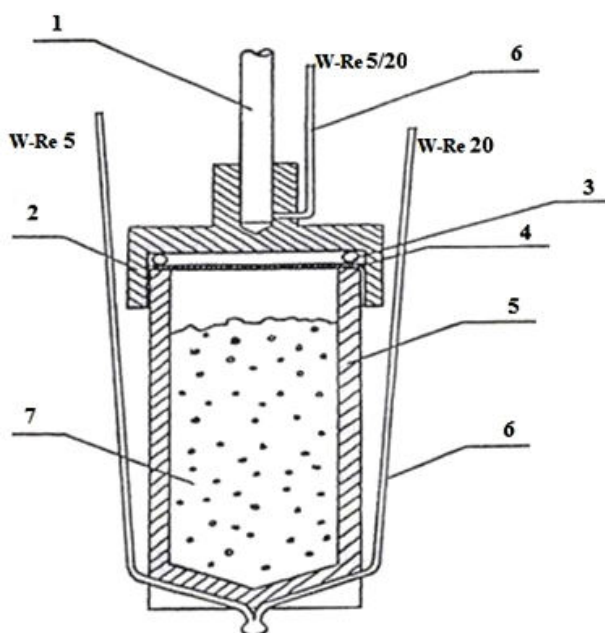


Fig. 2. DSC module: 1 – bearing tungsten rod; 2 – lid with a press-fit rod; 3 – gasket of tungsten wire; 4 – molybdenum plate; 5 – crucible; 6 – thermocouples; 7 – sample

where X_2 is the mole fraction of impurity in an ideal liquid phase; A is the first cryoscopic constant (K^{-1}); ΔT is the melting point depression with respect to a pure substance (K); ΔH_f is the fusion heat (enthalpy) of a pure substance (J/mol); R is the universal gas constant ($8.314 \text{ J/mol}\cdot\text{K}$); and T_0 is the melting point of a pure substance (K).

In the second approach, the Le Chatelier-Shreder equation was utilized [10]:

$$T = \frac{T_0}{\left(1 - \frac{\ln X_i}{N_i}\right)}, \quad (3)$$

where X_i is the mole fraction of the impurity component; and N_i is the number of atoms in the formula of a compound.

The calculated liquidus temperatures using equations (1)–(3), based on data from different authors [5,9,10] for melting temperatures and enthalpies of formation of MnO and Al_2O_3 , determined for MnO and Al_2O_3 , are provided below (Table 3).

The maximum liquidus temperature calculated

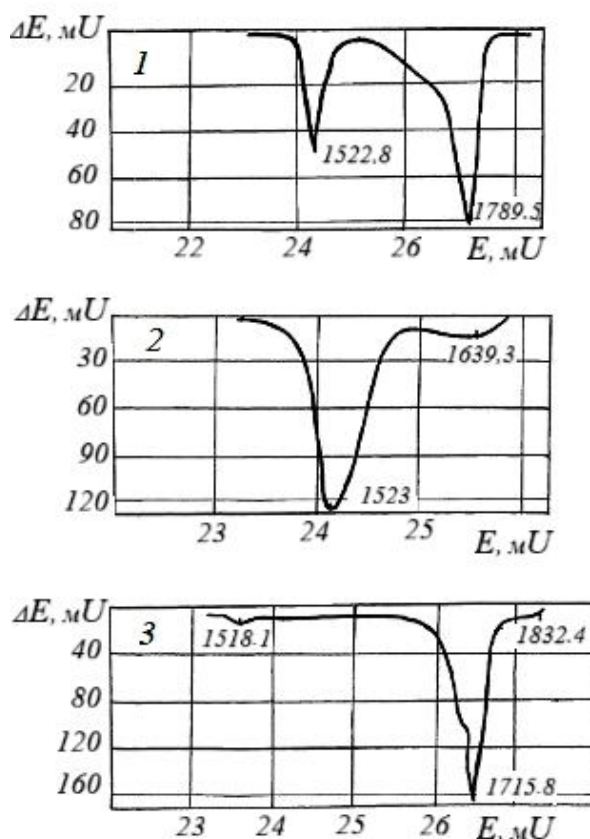


Fig. 3. DSC curves of samples No. 1, 2, and 3 (Table 2) in the $\text{MnO}-\text{Al}_2\text{O}_3$ system obtained during heating

using equation (3) coincides with the phase diagram [5]. However, the pattern of temperature change corresponds to its gradual increase with the Al_2O_3 content and aligns with the phase diagram [11–13].

The issue of whether the melting process of MnAl_2O_4 (as shown in Fig. 1) is congruent or incongruent is primarily related to the preservation of short-range structural bonds after melting. The preservation of short-range order (congruent melting) is attributed to the absence of a coordination rearrangement in the chemical compound during the isomorphic transformation near the melting temperature. According to data from [14,15], manganese spinels, such as MnTi_2O_4 , MnV_2O_4 , and MnAl_2O_4 , exhibit the same enthalpy of spinel formation from oxides, which is equal to 38.5 kJ/mol. The enthalpy of formation for MnAl_2O_4 spinels, obtained calorimetrically, closely agrees with the calculated enthalpy of formation from oxides. This agreement suggests the retention of the coordination number of manganese and aluminum cations, which is characteristic of both oxides. In manganese spinels, manganese occupies octahedral positions with a coordination number of $\text{CN}(\text{Mn})=6$, corresponding to pure MnO . The coordination number of aluminum in Al_2O_3 varies from six- to four-coordinated since aluminum cations occupy octahedral and tetrahedral positions in $\alpha\text{-Al}_2\text{O}_3$. In spinels,

aluminum cations are found in both octahedral and tetrahedral positions. Therefore, the prevailing nature of MnAl_2O_4 melting is congruent.

Conclusions

The conducted research indicates a congruently melting nature of manganese spinel MnAl_2O_4 , which aligns with the experimental data from ref. [2]. The preservation of short-range order during the melting of MnAl_2O_4 affects the thermodynamic stability parameters of the compound and the temperature at the onset of manganese recovery during carbothermic reduction. The congruent melting of manganese spinel implies the presence of a second eutectic E2, positioned between MnAl_2O_4 and Al_2O_3 . According to experimental data, the melting temperature of eutectic E2 is lower, approximately at 1720°C, which coincides with the data from ref. [5].

REFERENCES

1. Gladkykh V.A., Ruban A.V., Gasyk M.I. Analiz rastvorimosti ugleroda v troinoi sisteme Mn–Si–C // Modern Problems of Metallurgy. – 2016. – Vol.19. – P.226-233.
2. Phase diagrams of refractory oxide systems and microstructural design of materials / Dudnik E.V., Lakiza S.N., Tishchenko Ya.S., Ruban A.K., Red'ko V.P., Shevchenko A.V., et al. // Powder Metall. Met. Ceram. – 2014. – Vol.53. –

Table 2

Experiment parameters, estimated temperatures, and the nature of transformations in the $\text{MnO}(\text{Mn})\text{--Al}_2\text{O}_3(\text{A})$ system

Sample No.	Composition, wt%. Test parameters	Temperature (°C), transformation characteristics		
1	90% MnO; 10% Al_2O_3			
	Heating: 980°C→1960°C Vheating=15 mV/h	1522.8	1789.5	
		Mn+E1→Mn+liquid	Mn+liquid→liquid	
	Cooling: 1960°C→980°C Vcooling=15 mV/h	1518.8	1778.2	
		Mn+liquid→Mn+E1	liquid→Mn+liquid	
2	78.2% MnO; 21.8% Al_2O_3			
	Heating: a) 1290°C→1810°C Vheating=15 mV/h	1523.0–1519.0	1639.3–1637.1	
	b) 1350°C→1720°C Vheating=5 mV/h	Mn+E1→Mn+liquid	Mn+liquid→liquid	
	Cooling: a) 1810°C→1350°C Vcooling=15 mV/h	1522.8–1521.3	1639.4–1641.7	
	b) 1720°C→1400°C Vcooling=5 mV/h	Mn+liquid→Mn+E1	liquid→Mn+liquid	
3	41% MnO; 59% Al_2O_3	1518.1	1715.8	1832.4
	Heating: 1180°C→1930°C Vheating=15 mV/h	MnA+E1→	MnA+liquid→	A+liquid→
		MnA+liquid	A+liquid	liquid
	Cooling: 1930°C→1180°C Vcooling=15 mV/h	1516.2	1715.8	1792.1
		MnA+liquid→	A+liquid→	liquid→A+
		MnA+E1	MnA+liquid	+liquid

P.303-311.

3. *Aramaki S., Roy R.* Revised phase diagram for the system $\text{Al}_2\text{O}_3\text{--SiO}_2$ // *J. Am. Ceram. Soc.* – 1962. – Vol.45. – P.229-242.

4. *Gasik M., Dashevskii V., Bizhanov A.* Ferroalloys: theory and practice. – Springer Cham, 2020. – 531 p.

5. *Gasik M., Gladkikh V.* Prediction of structure and assessment of the phase transformation direction in melts of the $\text{MnO--SiO}_2\text{--CaO--MgO--Al}_2\text{O}_3$ system. *Manganese metallurgy*. – M.: MGUP «Eutectics», 1991. – P.17-18.

6. *Gladkikh V., Lysenko V., Chepelenko O.* Promyslova vyplavka sylikomarhantsiu z vykorystanniam u shykhti shlakovuhilnykh bryketiv // *Fyzykokhimichni Doslidzhennia Metalovidkhodnykh Protsesiv v Elektrotermii*. – 1985. – P.91-96.

7. *Gasik M., Gladkikh V.* The investigation of phosphorus chemical bond. In: *The manganese-ore materials. Energy efficiency and environmental friendliness are the future of the global ferroalloy industry* // *Proceedings of the fourteenth international ferroalloys congress Infacon XIV*. – 2015. – P.470-478.

8. *Proidak Yu., Gladkykh V., Ruban A.* Studying the phase equilibria in MnO--SiO_2 system by the differential scanning calorimetry (DSC) method // *Science and Innovation*. – 2022. – Vol.18. – No. 2. – P.100-107.

9. *Ore melting and reduction in silicomanganese production* / Ringdalen E., Gaal S., Tangstad M., Ostrovsky O. // *Metall. Mater. Trans. B*. – 2010. – Vol.41. – P.1220-1229.

10. *Roghani G., Jak E., Hayes P.* Phase equilibrium studies in the « $\text{MnO--Al}_2\text{O}_3\text{--SiO}_2$ » system // *Metall. Mater. Trans. B*. – 2002. – Vol.33. – P.827-838.

11. *Gasik M.* Handbook of ferroalloys: theory and technology. – Elsevier, 2013. – 419 p.

12. *Chatterjee S., Jung I.-H.* Critical evaluation and thermodynamic modeling of the Al--Mn--O ($\text{Al}_2\text{O}_3\text{--MnO--Mn}_2\text{O}_3$) system // *J. Eur. Ceram. Soc.* – 2014. – Vol.34. – P.1611-1621.

13. *Shuvaiev S., Proidak Yu., Gasik M.* Renthenostrukturne doslidzhennia marhantsevykh kontsentrativ zbahachennia syroi rudy ta shlamu vidpratsovanoho shlamonakopychuvacha metodom intensyvnoi mokroi mahnitnoi separatsii // *Metalurhiina ta Hirnychorudna Promyslovist*. – 2017. – No. 4. – P.13-18.

14. *The determination of rational technological parameters of ferrosilicon manganese melting based on the process electrical characteristics. Energy efficiency and environmental friendliness are the future of the global ferroalloy industry* / Ruban A.V., Kutsin V.S., Gladkikh V.A., Olshansky V.I., Filippov I.Yu., Kyzmenko S.M., et al. // *Proceedings of the fourteenth international ferroalloys congress Infacon XIV*. – 2015. – Vol.1. – P.107-114.

15. *Ruban A.V., Gladkikh V.A., Kutsin V.S.* Termodynamichne ta eksperymentalne vyznachennia temperaturnykh umov rivnovahy metalevoi ta oksydnoi faz pry sumisnomu vidnovleni oksydiv marhantsiu ta kremniiu vuhletsem // *Teoriia i Praktyka Metalurhii*. – 2019. – No. 2. – P.29-33.

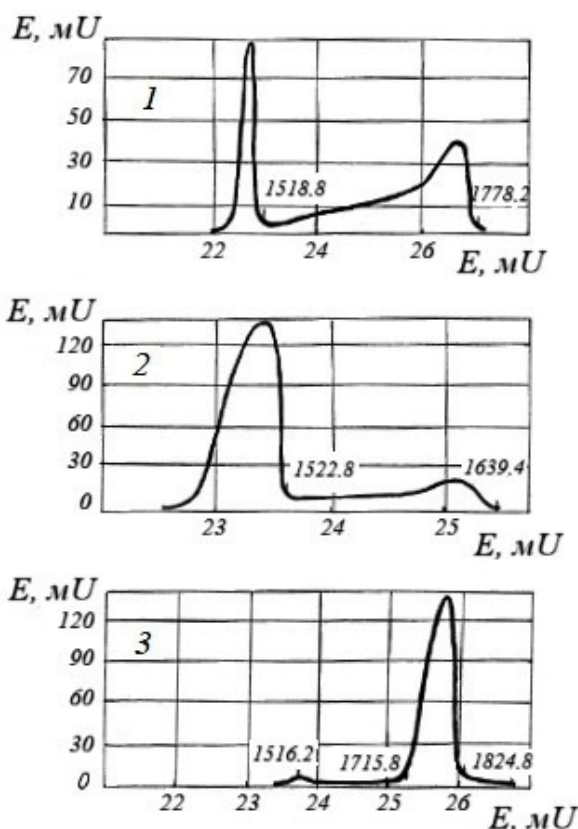


Fig. 4. DSC curves of samples No. 1, 2, and 3 (Table 2) in the $\text{MnO--Al}_2\text{O}_3$ system obtained during cooling

Table 3

Calculated liquidus temperatures in the $\text{MnO--Al}_2\text{O}_3$ system

Composition, mol.%	Temperature, °C	
	Eq. (2)	Eq. (3)
45% MnO	1867	1792
50% MnO	1846	1767
55% MnO	1826	1732

Received 12.11.2024

ДОСЛІДЖЕННЯ ФАЗОВИХ РІВНОВАГ У СИСТЕМІ $\text{MnO}-\text{Al}_2\text{O}_3$ МЕТОДОМ ДИФЕРЕНЦІАЛЬНОЇ СКАНУВАЛЬНОЇ КАЛОРИМЕТРІЇ**Ю.С. Пройдак, В.А. Гладких, А.В. Рубан, О.О. Рябцев**

Усі шлаки від виробництва марганцевих феросплавів можуть бути умовно віднесені до системи $\text{MnO}-\text{CaO}-\text{SiO}_2-\text{Al}_2\text{O}_3$, оскільки сумарний вміст цих оксидів сягає 95–98% при вмісті MnO від 18% до 48%. З практичної точки зору важливо знати особливості поведінки силікатних систем у широкому температурному діапазоні та за наявності різних домішок. Для вивчення концентраційно-температурних перетворень у розплавах, що відповідають марганцевому алюмінату, низькотемпературному евтектику E1 та марганцевмісній ділянці із вмістом 10% Al_2O_3 , було застосовано метод диференціальної сканувальної калориметрії. Проведені дослідження вказують на конгруентний характер плавлення марганцевої шпінелі MnAl_2O_4 . Збереження ближнього порядку під час плавлення MnAl_2O_4 впливає на параметри термодинамічної стабільності сполуки та температуру початку відновлення марганцю при карботермічному відновленні. Конгруентне плавлення марганцевої шпінелі передбачає наявність другої евтектики E2, розташованої між MnAl_2O_4 та Al_2O_3 . За експериментальними даними температура плавлення евтектики E2 є нижчою і становить приблизно 1720°C.

Ключові слова: марганцеві феросплави; фазова рівновага; система $\text{MnO}-\text{Al}_2\text{O}_3$; диференціальна сканувальна калориметрія; диференціальний термічний аналіз; шпінель.

INVESTIGATION OF PHASE EQUILIBRIA IN THE $\text{MnO}-\text{Al}_2\text{O}_3$ SYSTEM BY DIFFERENTIAL SCANNING CALORIMETRY METHOD**Yu.S. Proidak, V.A. Gladkykh, A.V. Ruban *, O.O. Riabtsev**
Ukrainian State University of Science and Technologies,
Dnipro, Ukraine

* e-mail: artem_ruban@ukr.net

All slag from the production of manganese ferroalloys can be conditionally attributed to the system $\text{MnO}-\text{CaO}-\text{SiO}_2-\text{Al}_2\text{O}_3$, since the sum of these oxides reaches 95–98% with MnO content from 18% to 48%. On the practical side, it is crucial to know the peculiarities of the behavior of silicate systems over a wide temperature range and in the presence of various additives. Differential scanning calorimetry was employed to study concentration–temperature transformations in melts corresponding to manganese aluminate, the low-temperature eutectic E1, and a manganese-rich region with 10% Al_2O_3 content. The conducted research indicates a congruently melting nature of manganese spinel MnAl_2O_4 . The preservation of short-range order during the melting of MnAl_2O_4 affects the thermodynamic stability parameters of the compound and the temperature at the onset of manganese recovery during carbothermic reduction. The congruent melting of manganese spinel implies the presence of a second eutectic E2, positioned between MnAl_2O_4 and Al_2O_3 . According to experimental data, the melting temperature of eutectic E2 is lower, approximately 1720°C.

Keywords: manganese ferroalloys; phase equilibrium; $\text{MnO}-\text{Al}_2\text{O}_3$ system; differential scanning calorimetry; differential thermal analysis; spinel.

REFERENCES

1. Gladkykh VA, Ruban AV, Gasyk MI. Analiz rastvorimosti ugleroda v troinoi sisteme Mn–Si–C [Analysis of carbon solubility in the ternary system Mn–Si–C]. *Modern Problems of Metallurgy*. 2016; 19: 226-233. (in Russian).
2. Dudnik EV, Lakiza SN, Tishchenko YaS, Ruban AK, Red'ko VP, Shevchenko AV, et al. Phase diagrams of refractory oxide systems and microstructural design of materials. *Powder Metall Met Ceram*. 2014; 53: 303-311. doi: 10.1007/s11106-014-9617-z.
3. Aramaki S, Roy R. Revised phase diagram for the system $\text{Al}_2\text{O}_3-\text{SiO}_2$. *J Am Ceram Soc*. 1962; 45: 229-242. doi: 10.1111/j.1151-2916.1962.tb11133.x
4. Gasik M, Dashevskii V, Bizhanov A. *Ferroalloys: theory and practice*. Springer Cham; 2020. 531 p. doi: 10.1007/978-3-030-57502-1.
5. Gasik M, Gladkikh V. *Prediction of structure and assessment of the phase transformation direction in melts of the $\text{MnO}-\text{SiO}_2-\text{CaO}-\text{MgO}-\text{Al}_2\text{O}_3$ system*. *Manganese metallurgy*. Moscow: MGUP «Eutectics»; 1991. p. 17-18.
6. Gladkikh V, Lysenko V, Chepelenko O. Promyslova vyplavka sylikomahantsiu z vykorystanniam u shykhti shlakovuhilnykh bryketiv [Industrial smelting of silicomarthrosis using slag briquettes]. *Fizykokhimichni Doslidzhennia Metalovidkhodnykh Protseviv v Elektrotermii*. 1985; 91-96. (in Ukrainian).
7. Gasik M, Gladkikh V. The investigation of phosphorus chemical bond. In: *The manganese-ore materials. Energy efficiency and environmental friendliness are the future of the global ferroalloy industry: Proceedings of the fourteenth international ferroalloys congress Infacon XIV*. May 31-June 4, 2015; Kyiv, Ukraine; 2015. p. 470-478.
8. Proidak Yu, Gladkykh V, Ruban A. Studying the phase equilibria in $\text{MnO}-\text{SiO}_2$ system by the differential scanning calorimetry (DSC) method. *Science and Innovation*. 2022; 18(2): 100-107. doi: 10.15407/scine18.02.100.
9. Ringdalen E, Gaal S, Tangstad M, Ostrovsky O. Ore melting and reduction in silicomanganese production. *Metall Mater Trans B*. 2010; 41: 1220-1229. doi: 10.1007/s11663-010-9350-z.
10. Roghani G, Jak E, Hayes P. Phase equilibrium studies in the $\text{MnO}-\text{Al}_2\text{O}_3-\text{SiO}_2$ system. *Metall Mater Trans B*. 2002; 33: 827-838. doi: 10.1007/s11663-002-0066-6.
11. Gasik M. *Handbook of ferroalloys: theory and technology*. Elsevier; 2013. 419 p. doi: 10.1016/c2011-0-04204-7.
12. Chatterjee S, Jung IH. Critical evaluation and thermodynamic modeling of the $\text{Al}-\text{Mn}-\text{O}$ ($\text{Al}_2\text{O}_3-\text{MnO}-\text{Mn}_2\text{O}_3$) system. *J Eur Ceram Soc*. 2014; 34: 1611-1621. doi: 10.1016/j.jeurceramsoc.2013.12.017.

13. Shuvaiev S, Proidak Yu, Gasik M. Renthenostrukturne doslidzhennia marhantsevykh kontsentrativ zbahachennia syroi rudy ta shlamu vidpratsovanoho shlamonakopychuvacha metodom intensyvnoi mokroi mahnitnoi separatsii [X-ray structural studies of manganese concentrates from the enrichment of raw ore and sludge from the processed sludge collector using the method of intensive wet vortex separation]. *Metalurhiina ta Hirnychorudna Promyslovist*. 2017; (4): 13-18. (in Ukrainian).

14. Ruban AV, Kutsin VS, Gladkikh VA, Olshansky VI, Filippov IYu, Kyzmenko SM, et al. The determination of rational technological parameters of ferrosilicon manganese melting based on the process electrical characteristics. Energy efficiency and environmental friendliness are the future of the global ferroalloy industry. *Proceedings of the fourteenth international ferroalloys congress Infacon XIV Volume 1*. 2015; Kyiv, Ukraine; 2015. p. 107-114.

15. Ruban AV, Gladkikh VA, Kutsin VS. Termodynamichne ta eksperymentalne vyznachennia temperaturnykh umov rivnovahy metalevoi ta oksydnoi faz pry sumisnomu vidnovleni oksydiv marhantsiu ta kremniiu vuhletsem [Thermodynamic and experimental determination of temperature conditions for the equilibrium of metal and oxide phases during the combined reduction of manganese oxide and silicon carbide]. *Teoriia i Praktyka Metalurhii*. 2019; (2): 29-33. (in Ukrainian).